Electronic Supplementary Material (ESI) for Catalysis Science & Technology.

Comparison of Two Multifunctional Catalysts [M/Nb_2O_5 (M=Pd, Pt)] for One-Pot Hydrodeoxygenation of Lignin

Supporting Information

1. Physical characterisation of the catalysts and extracted lignin.

Table S1. GPC analysis of isolated lignin from birch wood.

Sample	M_w (g mol^{-1})	M_n (g mol^{-1})	M_w/M_n
Birch lignin	3214	1700	1.89

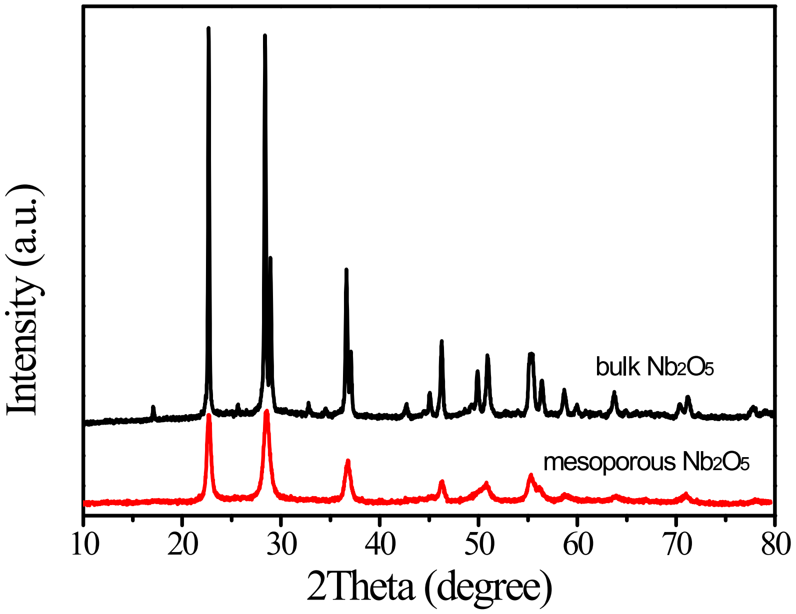

Figure S1. XRD patterns of mesoporous Nb_2O_5 and bulk Nb_2O_5.

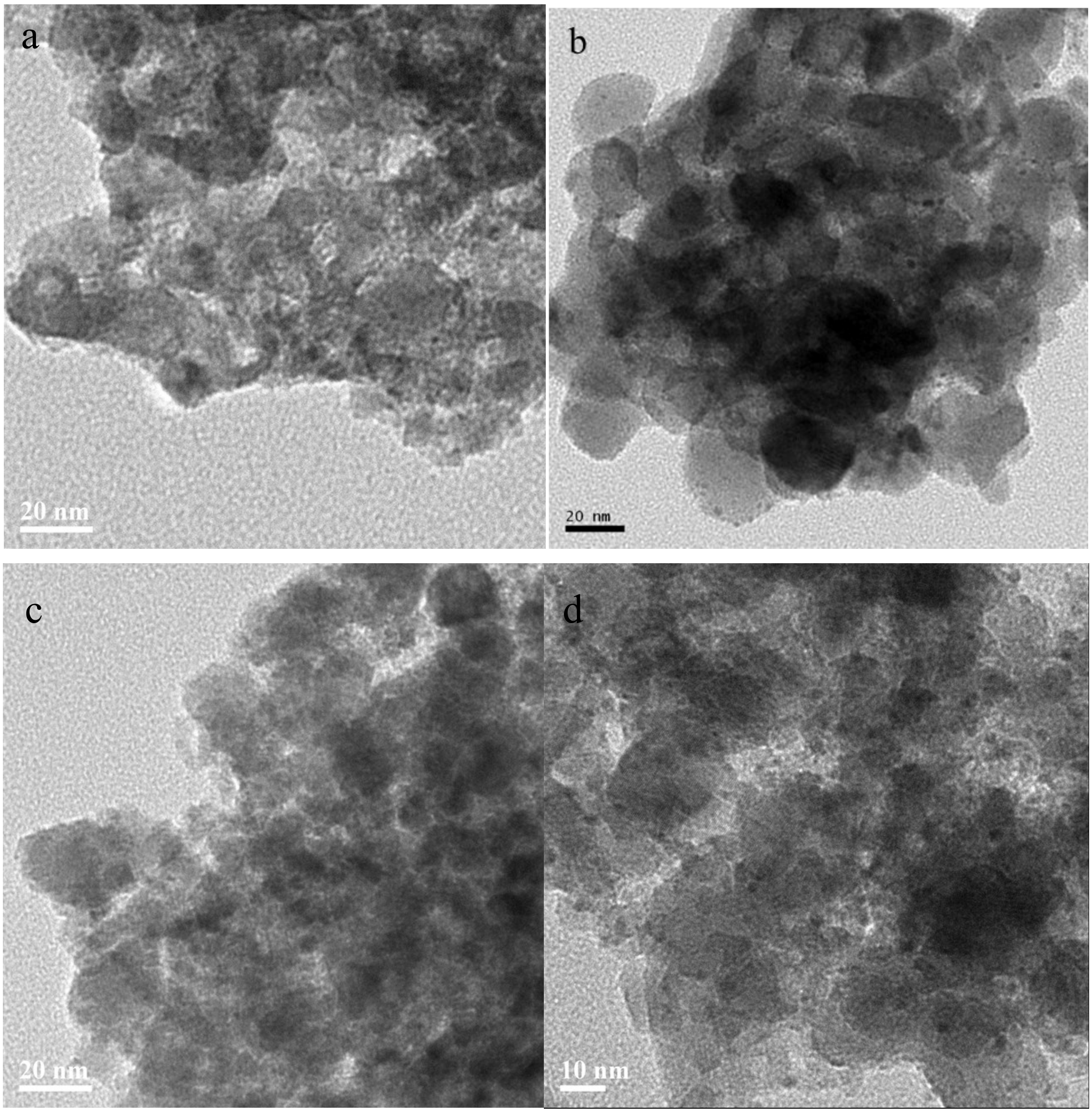

Figure S2. TEM images of fresh catalysts and used catalysts after four recycling runs: (a) Pd/Nb_2O_5, (b) Pt/Nb_2O_5, (c) used Pd/Nb_2O_5 and (d) used Pt/Nb_2O_5.

Table S2. Chemical composition of raw lignin before reaction.

Sample	Element content (wt%)				
	C	H	O	N	S
Birch lignin	64.8	7.3	27.9	0.1	0.0
Alkaline lignin	63.6	6.3	28.1	0.6	1.4

2. Analysis of lignin monomers by alkaline nitrobenzene oxidation method (NBO).

NBO was performed following a reported literature procedure.[3,4] In a typical reaction, extracted birch lignin (40 mg) was mixed with nitrobenzene (0.4 mL) and 2 M NaOH (7 mL) and reacted at 170°C for 2 h in an oil bath. Afterwards, the reactor was cooled in ice-water and 1 mL of freshly prepared ethyl vanillin (3-ethoxy-4-hydroxybenzaldehyde, **EV**) (5 μmol/mL) in 0.1 M NaOH solution was added to the reaction mixture as an internal standard. The mixture was transferred to a 100-mL separation funnel and washed three times with 15 mL of dichloromethane. The remaining aqueous layer was acidified with 2 M HCl, until the pH was below 3.0 and extracted twice with 20 mL of dichloromethane and 20 mL of diethyl ether. The combined organic layer was washed with deionised water (20 mL) and dried over Na_2SO_4. After filtration, the filtrate was collected in a 100-mL pear-shaped flask and dried under reduced pressure. For the TMS (trimethylsilyl) derivatisation step, NBO-products were washed with pyridine (3 × 200 μL) into a GC vial and BSTFA (150 μL) was added. The mixture was heated to 50 °C for 30 min. The silylated NBO-products were analyzed by GC-MS (Agilent 7890A GC-MS) equipped with aHP-5 capillary column (30 m × 250 μm) to identify the products by the comparison with the peak retention time and mass spectra of the authentic compounds. The identified products were quantified by GC-FID (Agilent 7890B) using the same column. Initial column temperature: 150°C (held for 10 min), raised at 5 °C/min to 280 °C (held for 20 min).

In the reported lignin upgrading reaction, the total yields of C_7~C_9 hydrocarbons on Pd/Nb_2O_5 (25.1 wt%, 2020 μmol/g lignin) and Pt/Nb_2O_5 catalysts (28.2 wt%, 2335 μmol/g lignin) were comparable with the yield of 2741 μmol/g lignin obtained through nitrobenzene oxidation (NBO) method (Figure S3), which is an established lignin monomer analysis method. This indicates that the total yields of C_7~C_9 hydrocarbons here is close to the theoretical yield.

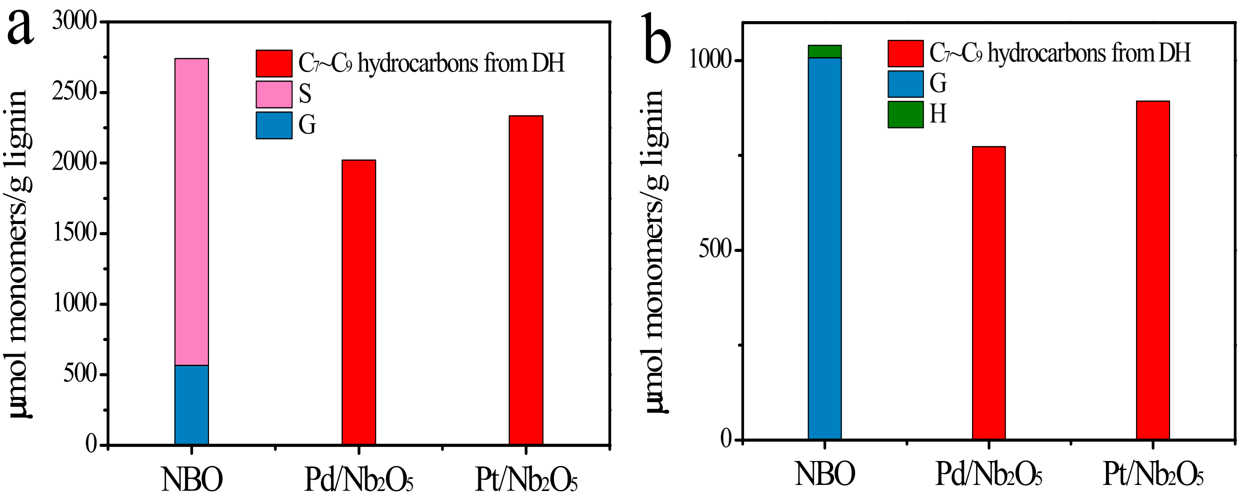

Figure S3. Analysis of (a) birch lignin and (b) alkaline lingnin monomer. "NBO" refers to the nitrobenzene oxidation method; "DH" refers to direct hydrogenolysis; "S" refers to syringy units; "G" refers to guaiacyl units.

3. Stability test

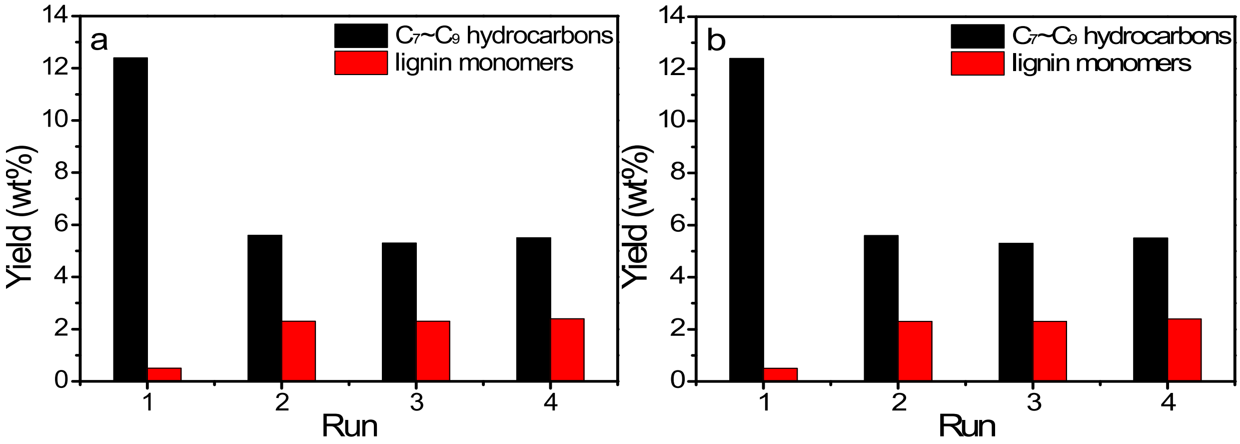

Figure S4 Recycling tests of lignin conversion over (a) Pd/Nb_2O_5 and (b) Pt/Nb_2O_5 catalysts with substrate (0.1 g)/catalyst (0.1 g) ratio. Reaction conditions: lignin 0.1 g, catalyst 0.1 g, 0.1 g, H_2O 15 mL, 250 °C, H_2 0.7 MPa, 20 h, stirring at 1000 rpm.

Table S3. Summary of product distribution from recycling tests of birch lignin conversion over Pd/Nb_2O_5 and Pt/Nb_2O_5.[a]

		Products distribution (wt%)							Total mass Yield (wt%)
		C_7~C_9 arenes			C_7~C_9 cycloalkanes				
Catalyst	Recycling	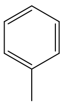	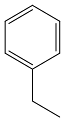	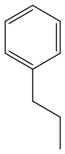	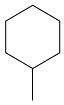	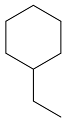	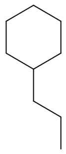	Lignin monomers[b]	
Pd/Nb_2O_5	Run 1	0.0	0.1	0.8	0.1	3.4	8.0	0.5	12.4
Pd/Nb_2O_5	Run 2	0.0	0.1	0.5	0.1	1.9	3.1	2.3	8.0
Pd/Nb_2O_5	Run 3	0.0	0.1	0.4	0.1	1.9	2.9	2.3	7.7
Pd/Nb_2O_5	Run 4	0.0	0.1	0.5	0.1	1.9	2.9	2.4	7.9
Pt/Nb_2O_5	Run 1	0.1	1.4	1.4	0.2	6.1	4.1	0.5	13.8
Pt/Nb_2O_5	Run 2	0.1	0.4	0.4	0.2	3.2	2.1	2.0	8.4
Pt/Nb_2O_5	Run 3	0.1	0.5	0.5	0.3	3.3	2.1	2.1	8.9
Pt/Nb_2O_5	Run 4	0.1	0.4	0.5	0.2	3.1	2.2	1.9	8.4

[a] Reaction conditions: lignin 0.1 g, catalyst 0.1g, H_2O 15 mL, 250 °C, H_2 0.7 MPa, 20h, stirring at 1000 rpm. The metal loading in each catalyst was at 2 wt%.
[b] The lignin monomers contain C_7-C_9 monocyclic oxygenated compounds and hydrocarbons.

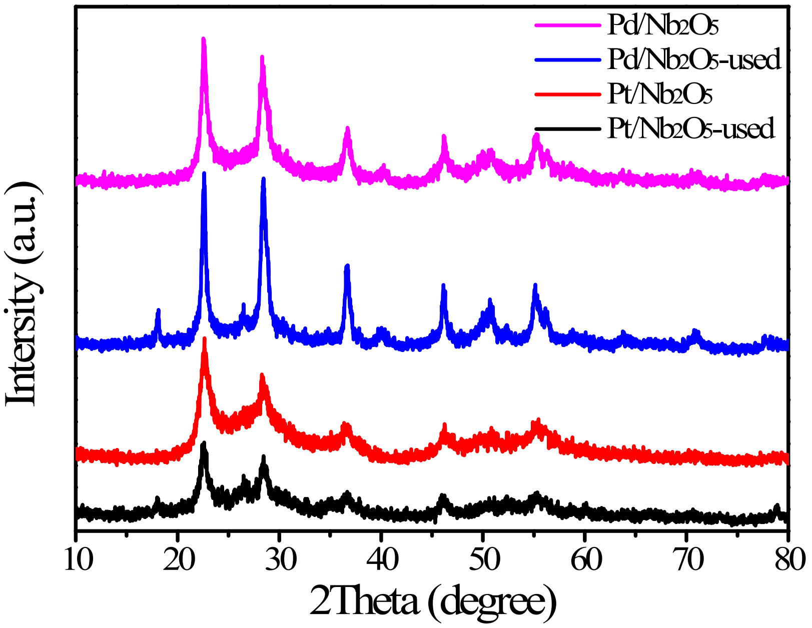

Figure S5. XRD patterns of fresh catalysts and used catalysts after four recycling runs.

4. Additional catalysis data.

Table S4. Summary of product yields from direct hydrodeoxygenation of birch lignin over Pd/Nb_2O_5 and Pt/Nb_2O_5 with different substrate/catalyst ratios.[a]

Catalyst	Amount of catalyst (g)	Products distribution (wt%)									Total mass Yield (wt%)/(C %)
		C_7~C_9 arenes			C_7~C_9 cycloalkanes						
		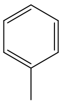	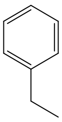	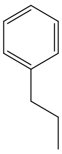	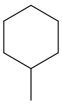	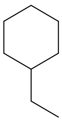	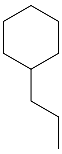	Other C_7~C_9[b]	C_{10}~C_{15}[c]	Others[d]	
Pd/Nb_2O_5	0.2g	0.2	0.4	1.7	3.3	7.4	10.4	1.7	3.7	3.1	31.9/42.2
Pd/Nb_2O_5	0.1g	0.0	0.1	0.8	0.1	3.4	8.0	0.1	0.3	0.1	12.9/17.1
Pt/Nb_2O_5	0.2g	0.2	1.5	2.1	1.8	10.4	11.2	1.0	3.0	3.5	34.7/46.1
Pt/Nb_2O_5	0.1g	0.1	1.4	1.4	0.2	6.1	4.1	0.1	0.2	0.2	13.9/18.5

[a] Reaction conditions: lignin 0.1 g, H_2O 15 mL, 250 °C, H_2 0.7 MPa, 20h, stirring at 1000 rpm. The metal loading in each catalyst was at 2 wt%.

[b] 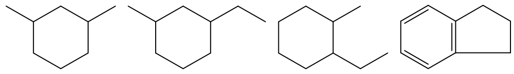

[c] 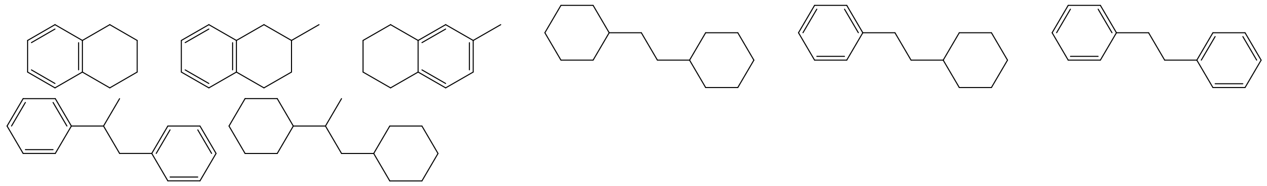

[d] C_{16} and C_{17} aliphatic alkanes and other products were only quantified by GC but not confirmed for structures.

Table S5. Summary of product yields from direct hydrodeoxygenation of alkaline lignin.[a]

Catalyst	Products distribution (wt%)									Total mass Yield (wt%)/(C%)
	C_7~C_9 arenes			C_7~C_9 cycloalkanes						
	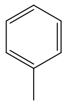	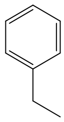	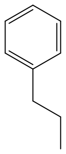	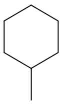	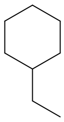	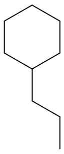	Other C_7~C_9[b]	C_{10}~C_{15}[c]	Others[d]	
Pd/Nb_2O_5	0.1	0.2	0.7	1.1	2.7	4.2	0.5	1.5	1.1	12.1/16.3
Pt/Nb_2O_5	0.1	0.5	0.9	0.6	4.2	4.1	0.3	1.1	1.2	13.0/17.6

[a] Reaction conditions: lignin 0.1 g, catalyst 0.2 g, H_2O 15 mL, 250 °C, H_2 0.7 MPa, 20h, stirring at 1000 rpm. The metal loading in each catalyst was at 2 wt%.

[b] 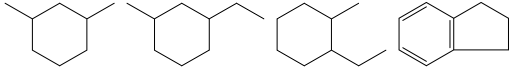

[c] 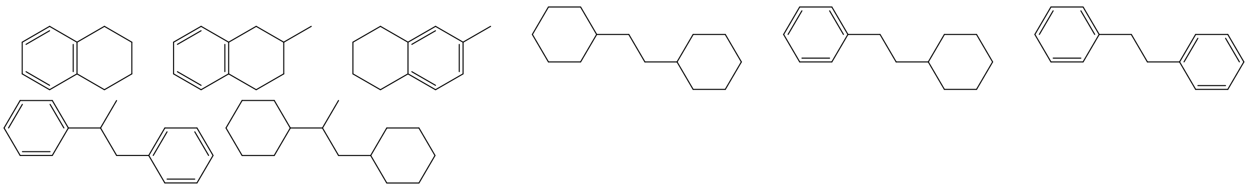

[d] C_{16} and C_{17} aliphatic alkanes and other products were only quantified by GC but not confirmed for structures.

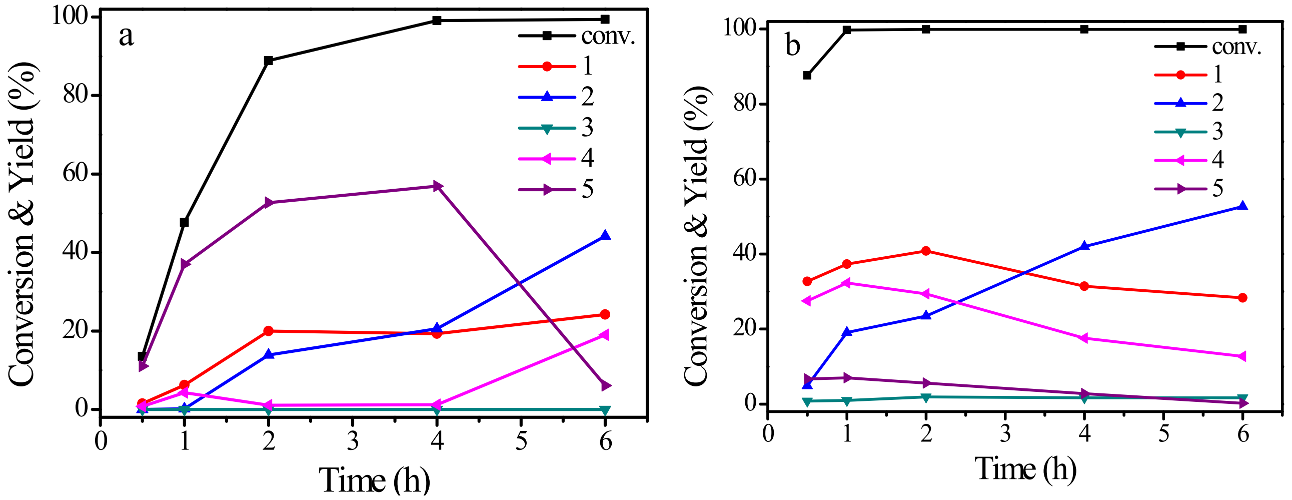

Figure S6. Products distribution for the conversion of 4-methylphenol over Pd/Nb_2O_5 (a) and Pt/Nb_2O_5 (b) catalysts as a function of time. Reaction conditions: substrate 0.2 g, catalyst 0.4 g, H_2O 15 mL, 250 °C, H_2 0.5 MPa, stirring at 1000 rpm.

5. *In situ* inelastic neutron scattering (INS) and DFT calculations

INS spectra were recorded on the TOSCA spectrometer at the ISIS Facility at the STFC Rutherford Appleton Laboratory (UK) and on the VISION spectrometer at Spallation Neutron Source, Oak Ridge National Laboratory (USA). Both TOSCA and VISION are indirect geometry crystal analyser instruments that provide a wide dynamic range (16–4000 cm^{-1}) with resolution optimised in the 50–2000 cm^{-1} range. In this region TOSCA has a resolution of 1.25% of the energy transfer. All the INS spectra for the catalysis system were collected after the sample was cooled and stabilised at temperatures below 30 K.

Approximately 20 g of each catalyst was loaded into a flow type stainless steel cell. By heating at 300 °C under He flow for 3 hours, the trace amount of water that was adsorbed on the catalyst surface was removed. The activated catalyst was then reduced by heating under a H_2 flow at 150 °C for 3 hours. To study the reaction mechanism, phenol was used as a model compound and dosed into the sample cell by a He flow at 150 °C for 3 hours. This allowed the phenol to be adsorbed on the catalyst surface and the INS spectrum of the phenol adsorbed catalyst was collected after cooling to below 30 K. After the data collection, phenol/H_2 was introduced to the cell for 7 min at 150 °C for the catalytic reaction to occur. The exhaust gas was monitored continuously *via* mass spectrometry. A further reaction was carried out by feeding H_2 for an additional 0.5-2 hours at 150 °C. INS spectra of pure solid compounds for both starting material and reaction products were collected at 10 K. A flow chart experimental procedure for the INS experiment was been shown in Fig. S18.

DFT Simulation. DFT calculations of the INS spectra for solid phenol, benzene, cyclohexane, cyclohexanone and cyclohexanol were carried out using their corresponding crystal structures,[5] which can be directly related to the experimental INS spectra of the solid state compounds with no approximations other than the use of DFT eigenvectors and eigenvalues to determine the spectral intensities. The information was used to identify the modes of vibrational features in the experimental INS spectra. No abscissa scale factor was used throughout this report for INS calculations. The calculated INS spectrum shows the total transitions (up to 10 orders). The calculations used the Projector Augmented Wave (PAW) method[6,7] to describe the effects of core electrons, and the Perdew-Burke-Ernzerhof (PBE)[8] implementation of the Generalized Gradient Approximation (GGA) for the exchange-correlation functional. The energy cutoff for the plane-waves is 500 eV, the energy tolerance for electronic structure calculation is 10^{-4} eV, and the maximum force is below 0.01 eV/Å after structural relaxation.

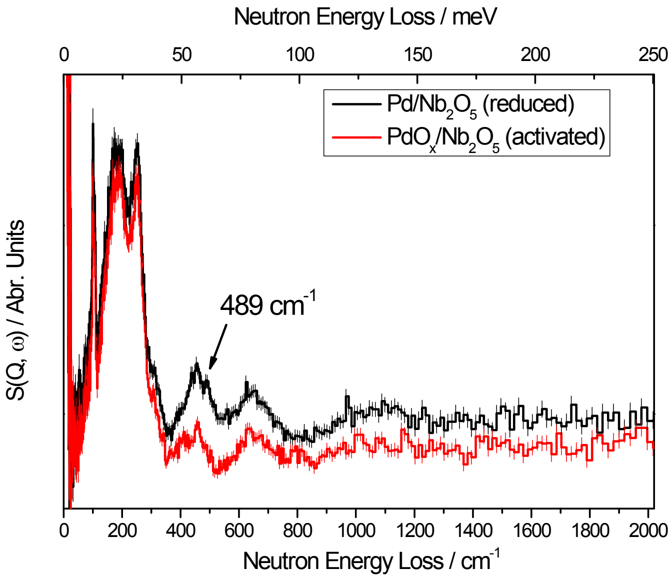

Figure S7. Comparison of INS spectra of the activated and reduced Pd/Nb_2O_5 catalyst.

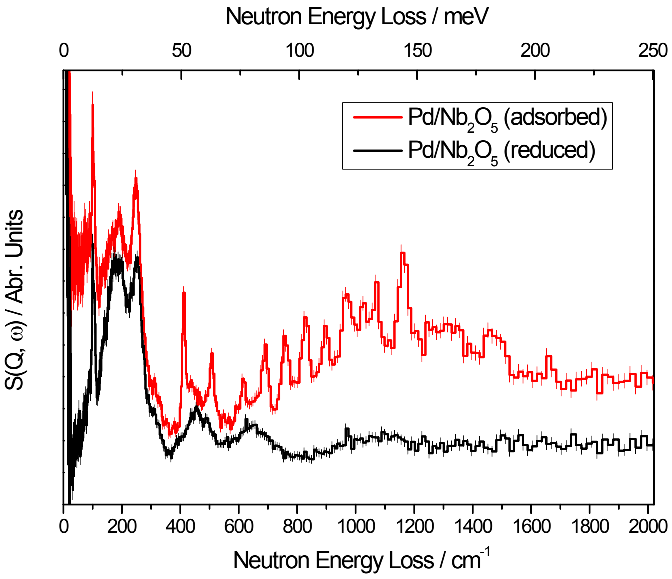

Figure S8. Comparison of the experimental INS spectra for bare Pd/Nb_2O_5 catalyst and the phenol adsorbed catalyst.

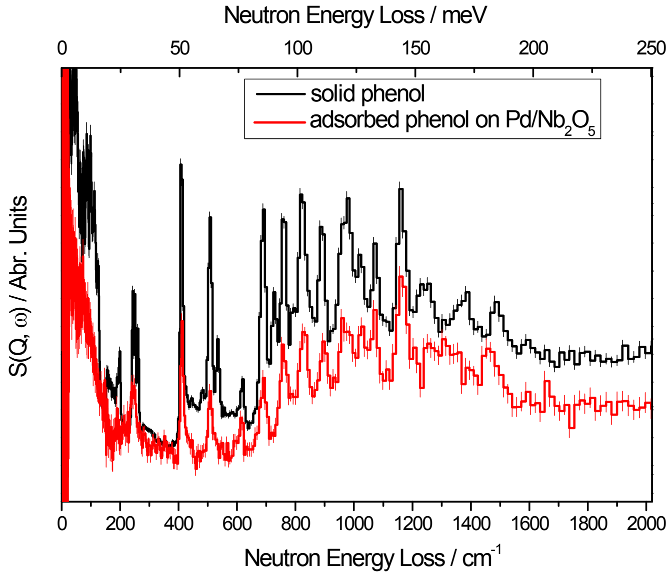

Figure S9. Comparison of the INS spectra of solid phenol and the phenol adsorbed on the Pd/Nb_2O_5 catalyst (obtained by subtracting INS spectrum of the reduced catalyst from the phenol adsorbed catalyst).

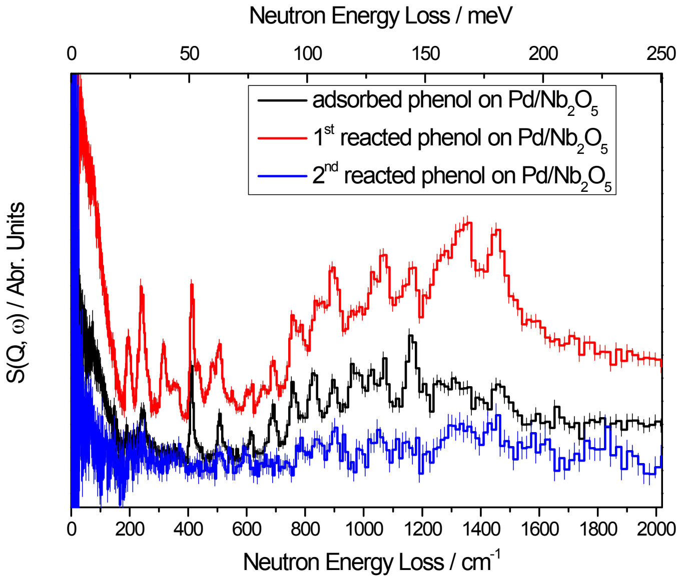

Figure S10. Comparison of INS spectra of the adsorbed, 1st and 2nd reacted phenol on the Pd/Nb_2O_5 catalyst.

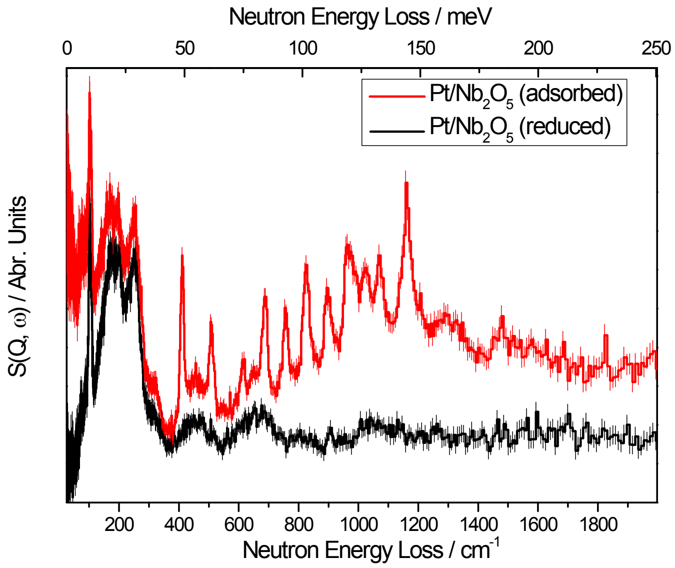

Figure S11. Comparison of the experimental INS spectra for bare Pt/Nb_2O_5 catalyst and the phenol adsorbed catalyst.

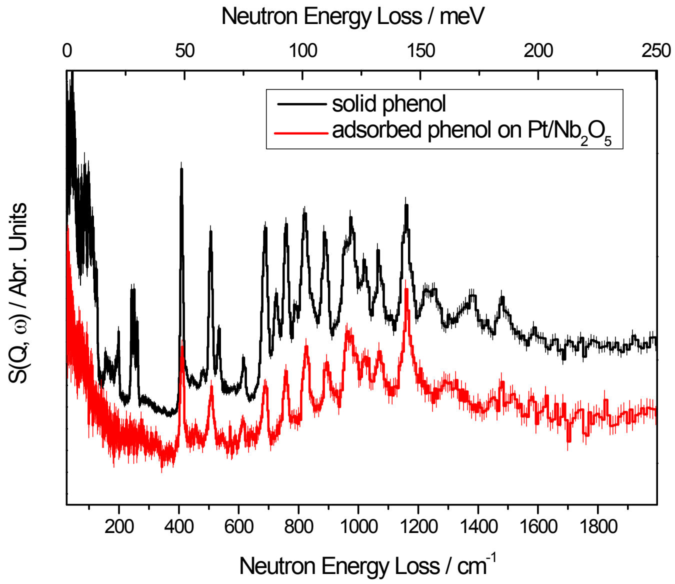

Figure S12. Comparison of the INS spectra of solid phenol and the phenol adsorbed on the Pt/Nb_2O_5 catalyst (obtained by subtracting INS spectrum of the reduced catalyst from the phenol adsorbed catalyst).

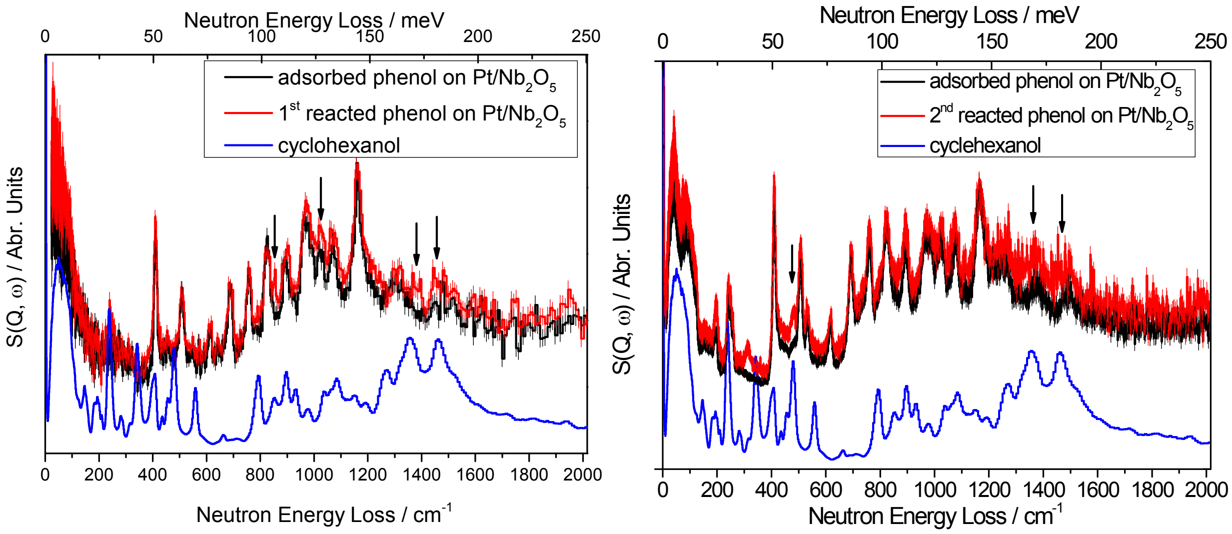

a b

Figure S13. Comparison of INS spectra of the adsorbed and 1st (a) and 2nd (b) reacted phenol on the Pt/Nb_2O_5 catalyst. INS spectrum of solid cyclohexanol is shown for reference. The black arrows indicate the increase of INS features that correlate with the formation of a small amount of cyclohexanol on the catalyst surface.

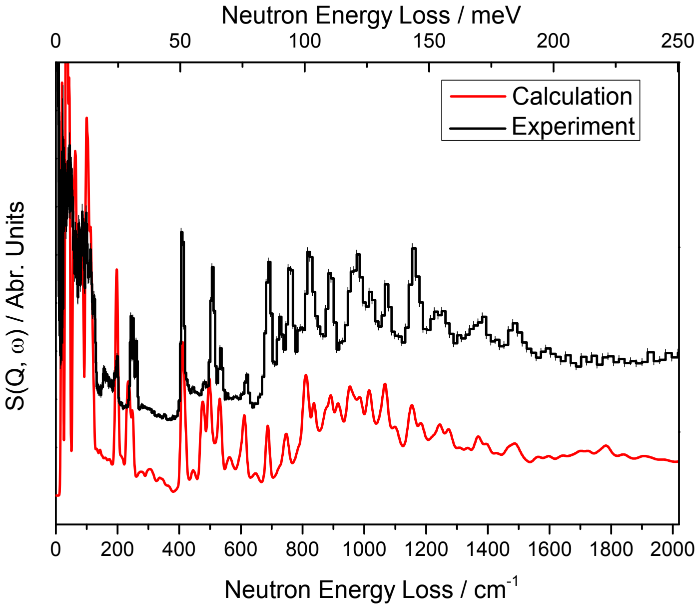

Figure S14. Comparison of calculated and experimental INS spectra of condensed phenol in solid at 10K.

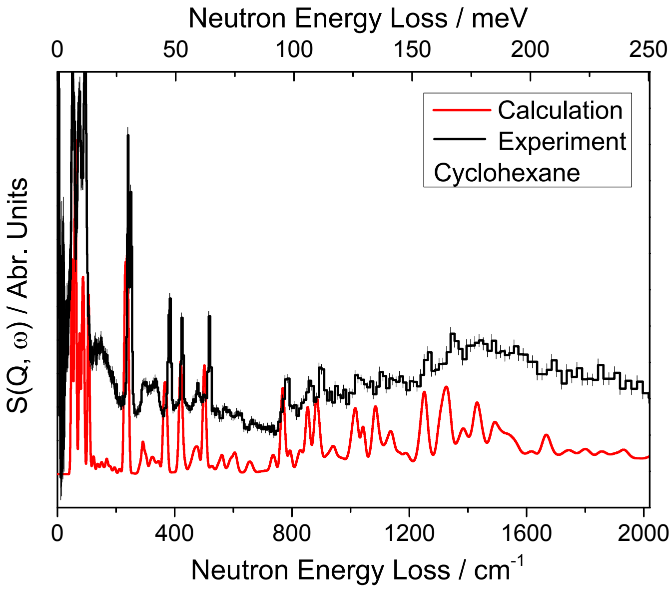

Figure S15. Comparison of calculated and experimental INS spectra of condensed cyclohexane in solid at 10K.

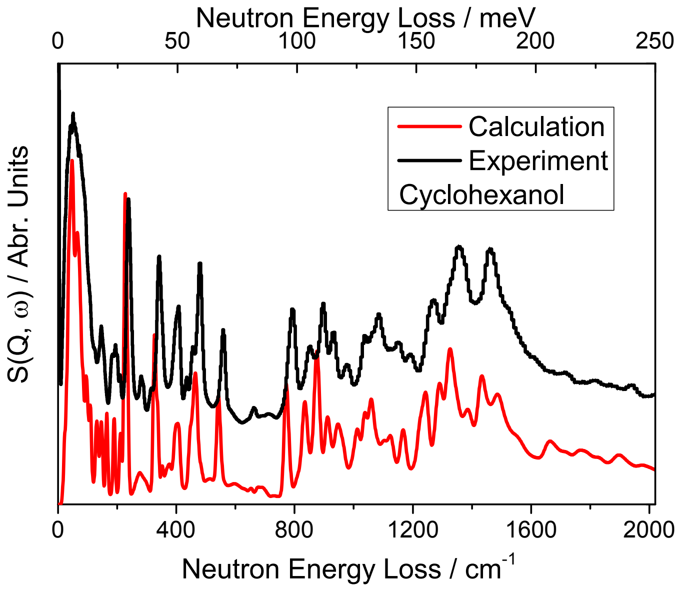

Figure S16. Comparison of calculated and experimental INS spectra of condensed cyclohexanol in solid at 10K.

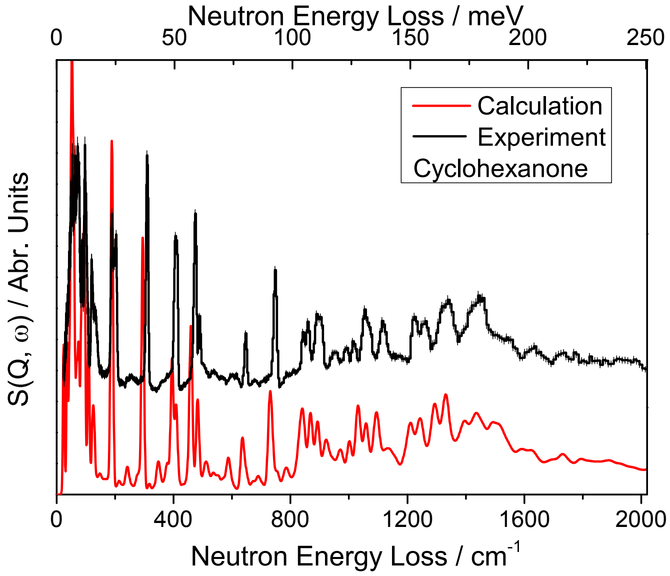

Figure S17. Comparison of calculated and experimental INS spectra of condensed cyclohexanone in solid at 10K.

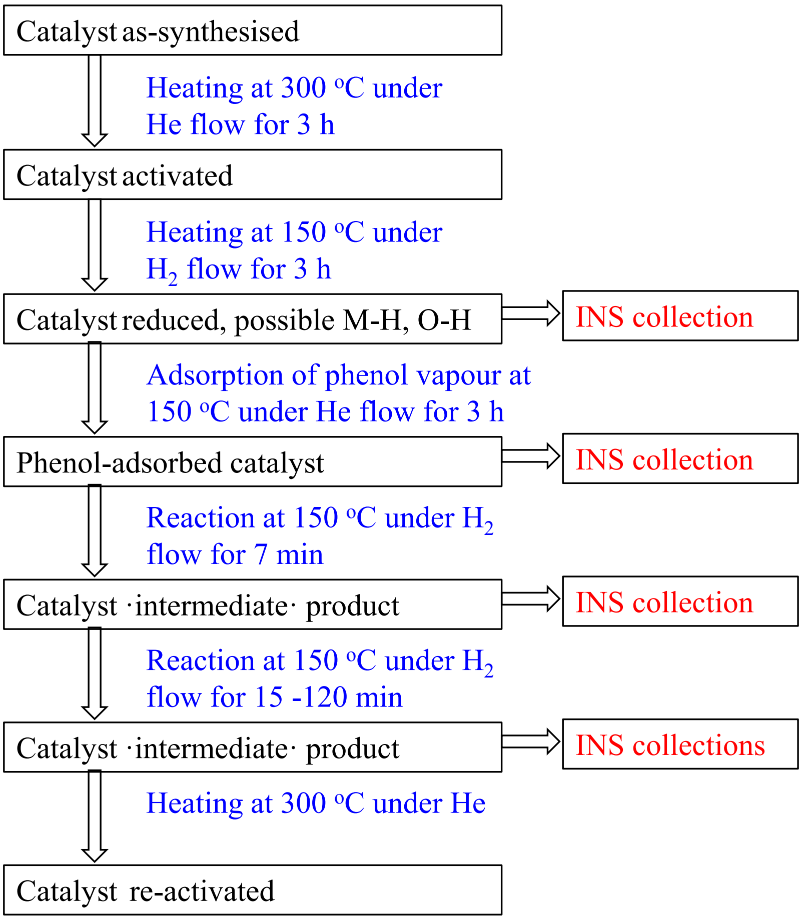

Figure S18. View of a flowchat for the *in situ* INS experiment. Two HDO reactions were carried out for phenol-adsorbed Pd/Nb_2O_5 at the time of 7 and 120 min. Three HDO reactions were conducted for phenol-adsorbed Pt/Nb_2O_5 at the time of 7, 15 and 120 min.

6. *In situ* Fourier Transform infrared spectroscopy (FTIR)

To further consolidate the conclusions, the in situ FTIR over Pd/Nb_2O_5 catalysts after phenol adsorption and reaction were also conducted (Fig. S19). Upon phenol adsorption at 150 °C, the appearance of many new spectral features were observed (3068、3035、1589、1490 and 1267 cm^{-1}), clearly demonstrating the binding of phenol molecules onto the catalyst surface. By comparing the difference spectrum and the FTIR spectra of gas-phase phenol (Fig. S20), a few changes were clearly observed. The intensity of the peak 1333cm^{-1} (assigned to vibration of the δ (OH)) was completely disappeared and the intensity of the peak 1267 cm^{-1} (assigned to vibration of the ν (CO) on phenoxide) was increased, suggesting that deprotonation of adsorbed phenol molecules to form phenoxide bound on the catalyst surface. The peaks at 1589 and 1490 cm^{-1} (assigned to the vibration of the ν ($C{=}C_{ring}$) on benzene ring) also concurrently shifted, suggesting that the adsorbed phenol molecules are disordered over the catalyst surface and have restricted translational motion owing to the strong binding to the catalyst. The FTIR spectra of the reaction system were collected after an phenol/H_2 stream flowing through the phenol adsorbed catalyst at 150 °C for 5 minutes, 10 minutes and 30 mimnutes. The intensity of the peaks at 1267 cm^{-1} was greatly decreased, while a new peak at 1670 cm^{-1} (assigned to the stretching vibration of the ν (C=O)) was formed. This observation indicates that the adsorbed phenol molecules underwent a 4-methylcyclohexanone as intermediate products and further conversion to produce 4-methylcyclohexanol and methylcyclohexane.

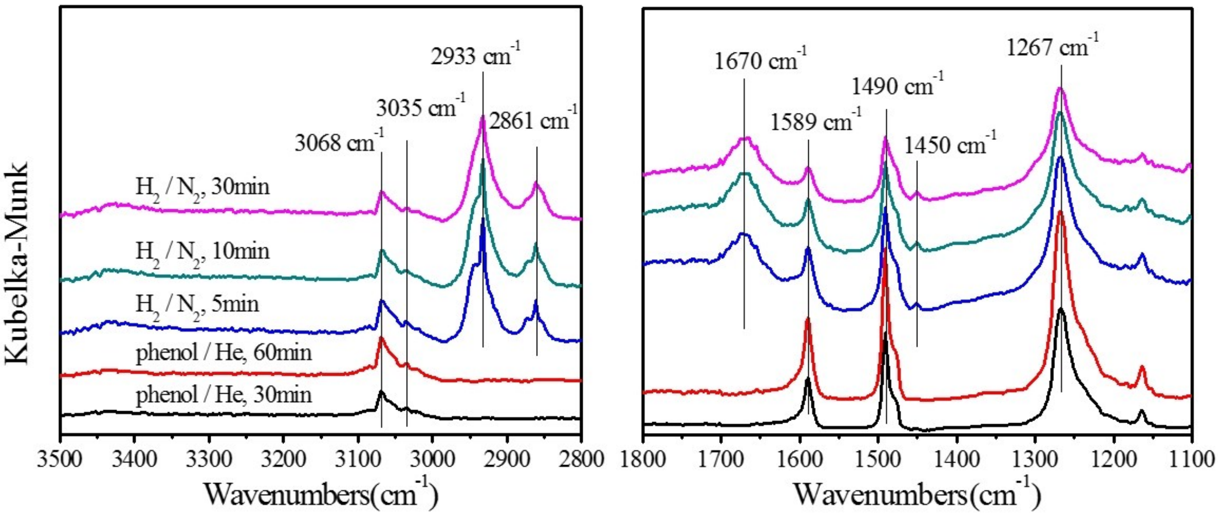

Figure S19. DRIFTS spectra obtained over Pd/Nb_2O_5 catalysts after phenol adsorption for 30 min and 60 min in a phenol/He flow, followed by purge with a 10%H_2/N_2 mixed gas for 5 min, 10 min and 30 min at 150 °C.

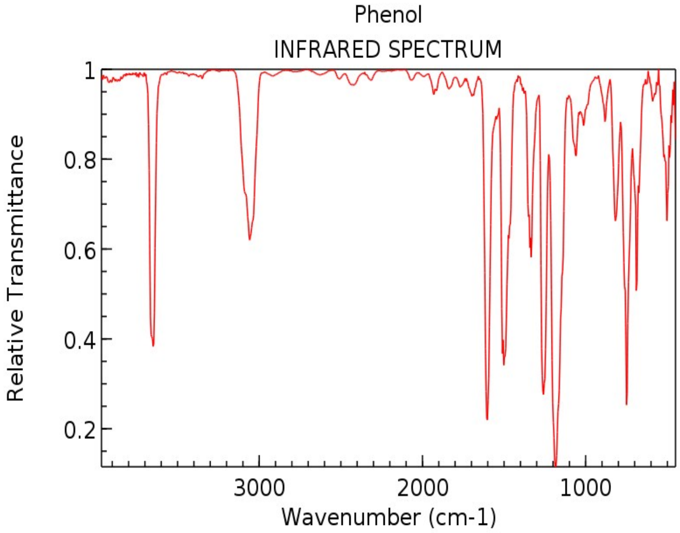

NIST Chemistry WebBook (http://webbook.nist.gov/chemistry)

Figure S20. FTIR spectra of gas-phase phenol from NIST Chemistry WebBook.

7. References

[1] Harris, E. E., D'Ianni, J. & Adkins, H. Reaction of hardwood lignin with hydrogen. *J. Am. Chem. Soc.* **60**, 1467-1470 (1938).

[2] Xia, Q. N., Cuan, Q., Liu, X. H., Gong, X. Q., Lu, G. Z., & Wang, Y. Q. Pd/$NbOPO_4$ multifunctional catalyst for the direct production of liquid alkanes from aldol adducts of furans. *Angew. Chem. Int. Ed.* **53**, 9755-9760 (2014).

[3] Shuai, L., Amiri, M. T., Questell-Santiago, Y. M, Héroguel, F., Li, Y., Kim, H., Meilan, R., Chapple, C., Ralph, J. Luterbacher, Jeremy S Formaldehyde stabilization facilitates lignin monomer production during biomass depolymerization. *Science* **354**, 329-333 (2016).

[4] Li, Y., Akiyama, T., Yokoyama, T. & Matsumoto, Y. NMR assignment for diaryl ether structures (4–O–5 structures) in pine wood lignin. *Biomacromolecules* **17**, 1921-1929 (2016).

[5] Kresse, G. and Furthmüller, J. Efficient iterative schemes for *ab initio* total-energy calculations using a plane-wave basis set. *Phys. Rev. B*, 54:11169 (1996).

[6] Blochl, P. E. Projector augmented-wave method. *Phys. Rev. B*, 50:17953 (1994).

[7] Kresse, G. and Joubert, D. From ultrasoft pseudopotentials to the projector augmented-wave method. *Phys. Rev. B*, 59:1758 (1999).

[8] Perdew, J. P., Burke K. and Ernzerhof, M. Generalized gradient approximation made simple. *Phys. Rev. Lett.*, **77**, 3865-3868 (1996).